Universiteit
Leiden
The Netherlands

Therapeutic targeting of immune escaped cancers

Marijt, K.A.

Citation
Marijt, K. A. (2020, February 18). *Therapeutic targeting of immune escaped cancers*. Retrieved from https://hdl.handle.net/1887/85450

Version:	Publisher's Version
License:	Licence agreement concerning inclusion of doctoral thesis in the Institutional Repository of the University of Leiden
Downloaded from:	https://hdl.handle.net/1887/85450

Note: To cite this publication please use the final published version (if applicable).

Cover Page

Universiteit Leiden

The handle http://hdl.handle.net/1887/85450 holds various files of this Leiden University dissertation.

Author: Marijt, K.A.
Title: Therapeutic targeting of immune escaped cancers
Issue Date: 2020-02-18

Chapter 5

Identification of non-mutated neoantigens presented by TAP-deficient tumors

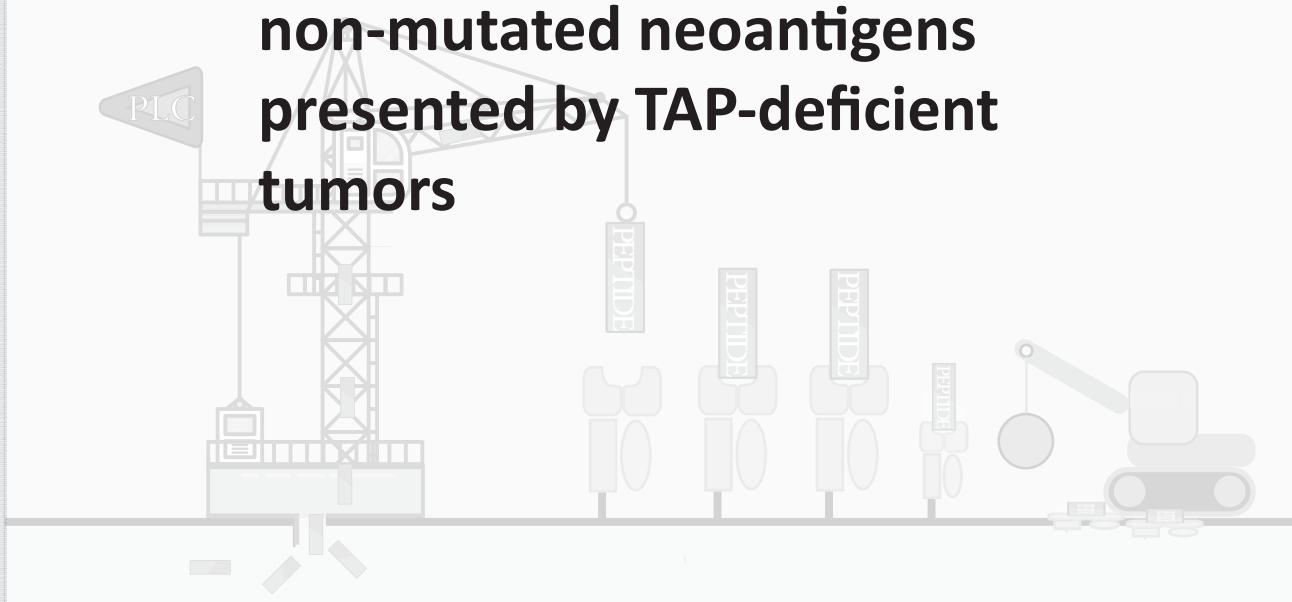

K. A. Marijt, *L. Blijleven, E. M. E. Verdegaal, M. G. Kester, D. J. Kowalewski, H. G. Rammensee, S. Stevanovic, M. H. M. Heemskerk, S. H. van der Burg and T. van Hall*

Journal of Experimental Medicine 215(9): 2325-2337 (2018)

Graphical abstract

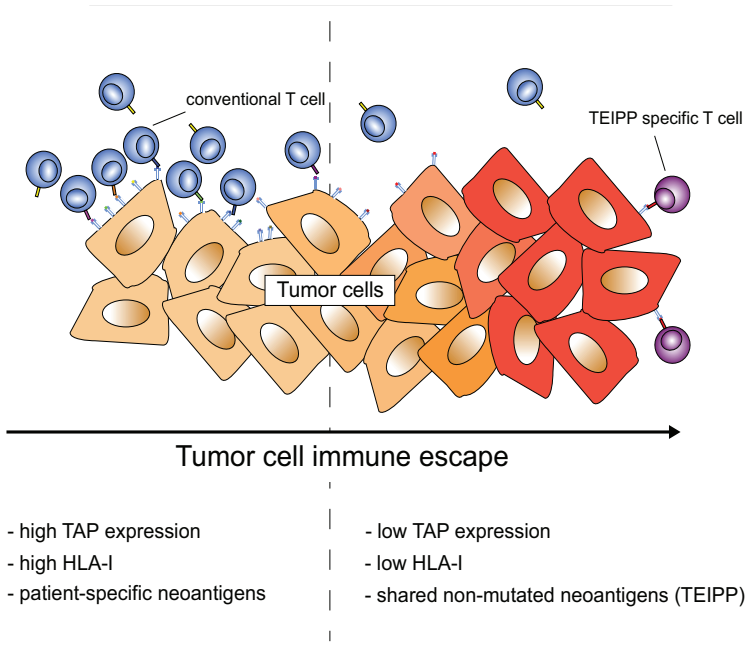

Most T-cell based immunotherapies of cancer depend on intact antigen presentation by HLA class I molecules (HLA-I). However, defects in the antigen processing machinery can cause down regulation of HLA-I, rendering tumor cells resistant to $CD8^+$ T cells. Previously, we demonstrated that a unique category of cancer antigens is selectively presented by tumor cells deficient for the peptide transporter TAP, enabling specific attack of such tumors without causing immunopathology in mouse models. With a novel combinatorial screening approach, we now identified 16 antigens of this category in humans. These HLA-A*02:01 presented peptides do not derive from the mutanome of cancers, but are of 'self' origin and therefore constitute universal neoantigens. Indeed, $CD8^+$ T cells specific for the leader-peptide of the ubiquitously expressed LRPAP1 protein recognized TAP-deficient, HLA-I^{low} lymphomas, melanomas, renal and colon carcinomas, but not healthy counterparts. In contrast to personalized mutanome-targeted therapies, these conserved neoantigens and their cognate receptors can be exploited for immune-escaped cancers across diverse histological origin.

Introduction

Many T-cell based immunotherapies for cancer are based on recognition of tumor antigens presented in human leukocyte antigen class I (HLA-I) molecules by tumor cells [1,2]. Success of immune checkpoint blockade therapy is strongly correlated with mutational load and mismatch repair deficient cancers, irrespective of tumor type [3,4]. Point mutated peptides indeed constitute formidable tumor antigens due to their non-self nature for which a non-curtailed T cell repertoire is available. An absolute requirement for such T cells to exert their action against cancer is the display of HLA-I at the surface of tumor cells. However, HLA-I down modulation on cancer cells is observed in many immune-escaped cancers, often caused by epigenetic silencing of antigen processing components, like the transporter associated with antigen processing (TAP) [5-7]. Recent studies implicated that acquired resistance to checkpoint therapy can occur through alterations in genes relevant for antigen processing and presentation [8,9]. For instance, mutations in the JAK1/JAK2 interferon signalling pathway represented acquired and primary resistance mechanisms in cancer patients who relapsed from or did not respond at all to checkpoint therapy, respectively. Notably, these mutations resulted in the inability to respond to interferon-**γ** (IFN-**γ**) and thus to upregulate antigen processing and presentation by HLA-I [10-12].

Our group previously discovered a novel category of tumor antigens, referred to as TEIPP (T cell epitopes associated with peptide processing), that are presented at the surface of tumor cells carrying defects in antigen processing [13]. In mouse tumor models in which MHC-I display is down modulated by defects in the peptide transporter TAP, we showed a selective presentation of TEIPP peptides, and successful targeting of immune-escaped tumor variants by TEIPP specific T cells [14,15]. Thus, targeting TEIPP neoantigens is a potent strategy to induce anti-tumor responses for tumors with low MHC-I expression. TEIPPs are derived from ubiquitously expressed non-mutated 'self' proteins, however, their processed peptides fail to be loaded into MHC-I in healthy cells. Their surface presentation is highly promoted by defects in the antigen processing machinery, especially in the absence of the peptide transporter TAP. Due to this virtue, TEIPP peptides constitute tumor-specific antigens. We have shown that the $CD8^+$ T cell repertoire against TEIPP neoantigens is positively selected in the thymus and that these cells remain naïve, even in tumor-bearing mice, making this subset fully exploitable for T-cell based therapies against immune-escaped cancers without any signs of autoimmune reactivity [15]. Yet, as to date only one human TEIPP neoantigen has been identified at the molecular level [16,17].

In order to identify multiple human TEIPP antigens, we developed a systematic hybrid forward-reversed immunology screen to identify human TEIPP antigens. This approach encompassed an *in silico* prediction of TEIPP neoantigen-candidates from the whole humane

proteome, matching of candidates to the cancer-specific peptidome, and an *ex vivo* screen to confirm the presence of a TEIPP T cell repertoire in healthy donors. Here, we present data on 16 identified HLA-A*02:01 binding TEIPP epitopes and a full characterization of the T cell reactivity against one of them.

Results

Strategy for target identification from the complete human proteome

To identify human TEIPP antigens that are presented by TAP-deficient cancer cells, we developed a hybrid forward-reversed immunology identification approach based on alternative antigen processing rules in combination with cancer-specific peptidome database matching (figure 1a). The whole human proteome was chosen as starting point, since TEIPP antigens are nonmutated 'self' antigens that are preferentially displayed on cells with deficiency in the peptide transporter TAP. This TAP-independent loading in HLA-I molecules can occur via two known alternative processing pathways: liberation of N-terminal 'signal peptides' and C-terminal 'tail peptides' [18-22] (figure 1a-b). A list of signal peptide-containing proteins was selected from the human proteome with the use of a web-based algorithm that predicts the signal peptidase (SP) cleavage site [23]. Most of these leader peptides need further processing by the proteolytic enzyme signal peptide peptidase (SPP) in order to release them from the endoplasmic reticulum (ER)-membrane and thereby generating peptides of different lengths suitable for loading in HLA-I [18,21]. This 'signal peptide' search yielded 111,525 different 9- and 10-mer TEIPP candidates. Additionally, C-terminal 'tail peptides' were selected using information on the topology of transmembrane proteins in the same web-based algorithm, knowing that liberation and TAP-independent processing of C-termini can be exerted by proteases like furin and SPP [20,24-27]. This search resulted in 6,674 'tail peptides' (figure 1a-b). Next, we filtered these combined peptides for a predicted high HLA-I binding-affinity (IC50<500 nM) to one of the so-called HLA 'supertypes', representing most alleles in the Caucasian population (HLA-A*01:01, HLA-A*02:01, HLA-A*03:01, HLA-B*07:02, HLA-B*40:01, HLA-A*24:02) [28-31]. This final list of 13,731 TEIPP candidates was then cross-matched with a large peptidome database, containing peptides eluted from over 200 tumor samples and 120 healthy tissue control samples (supplementary table I). Thereby, we focused on those TEIPP candidates that were endogenously processed and exclusively presented by tumor cells (figure 1c). This strategy yielded a short-list of 65 TEIPP neoantigen-candidates of which 40 had a predicted binding to the HLA-A*02:01 allele (supplementary figure 1a-d). These 40 HLA-A*02:01 binding peptides were chosen to explore the existence of cognate $CD8^+$ T cells (figure 1a).

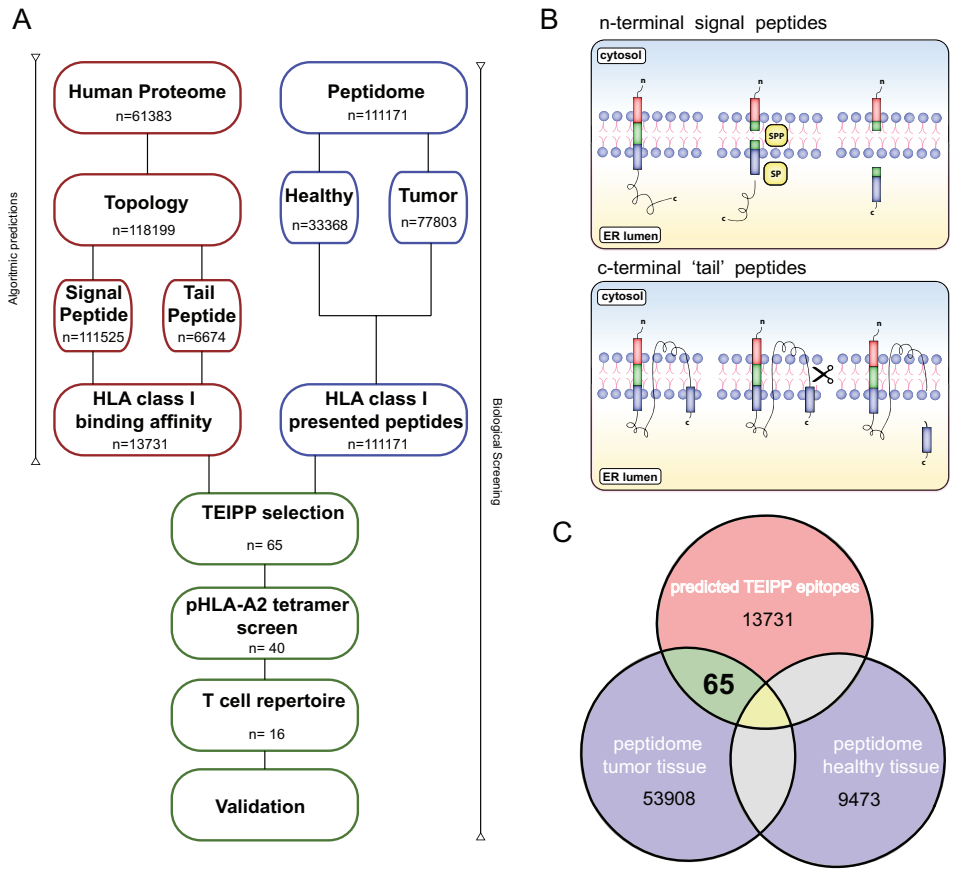

Figure 1: Identification approach of TEIPP neoantigens associated with immune-edited cancers

(**A**) A schematic overview of the applied screening approach. Human peptide sequences were selected via algorithms-based predictions on the whole human proteome for presentation by HLA-I molecules independent of the peptide transporter TAP. Two main unraveled pathways have been described for which algorithms are available: the processing of signal peptides and of C-terminal 'tail' peptides (*red*). The resulting peptide selection was matched with a large database of naturally presented peptides from human cancers and healthy tissue (*blue*). The subsequent shortlist of candidates with a predicted binding to HLA-A*02:01 was subjected to functional testing for T cell immunogenicity and recognition of tumor cells deficient for the peptide transporter (*green*). (**B**) Graphical display of the two molecularly described TAP-independent processing mechanisms. Top panel: Signal peptide containing proteins are processed in the ER membrane by the proteolytic enzymes signal peptidase (SP) and signal peptide peptidase (SPP), resulting in the liberation of small peptides in the lumen of the ER where they can bind to HLA class I molecules [18,53]. Bottom panel: Proteins with their C-terminal tail protruding in the ER can be cleaved by proteases like furins or SPP [20,26]. (**C**) Venn diagram of *in silico* predicted TEIPP neoantigens matched with databases comprising naturally presented peptides from tumor tissues or healthy tissues.

Detectable frequencies of CD8$^+$ T cells against 16 out of 40 HLA-A*02:01 binding TEIPP neoantigens

To validate that T cells against these TEIPP neoantigens were present in the repertoire of healthy donors, we grouped forty different HLA-A*02:01 tetramers containing the TEIPP neoantigens in eight pools of five peptides each, based on predicted binding affinity (high in 'peptide pool 1' to low in 'peptide pool 8'). Next, CD8$^+$ T cell cultures were started with tetramer-assisted 'pull-downs' from peripheral blood mononuclear cells (PBMC). These enriched CD8$^+$ T cell pools were stimulated with the five respective synthetic peptides of that particular pool for several rounds and analyzed for presence of peptide-specific T cells by flow cytometry (figure 2a). In an initial screen of three different HLA-A*02:01-positive healthy donors we observed T cell repertoires for 16 out of 40 TEIPP neoantigen candidates (figure 2a). Frequencies of tetramer-stained CD8$^+$ T cells varied from 0.1% up to 78% in these short-term expanded cultures. These percentages differed between the three tested donors, indicating that this protocol enabled the detection of TEIPP-specific CD8$^+$ T cells but that the observed frequencies reflected variation of the *in vitro* steps of enrichment and expansion. Additional donors were examined for the 16 positive peptides to evaluate the consistency of this finding and against most peptides CD8$^+$ T cells were detected, in the majority of the donors (figure 2b and Table 1). Collectively, these data indicated that our TEIPP identification strategy had a high success rate to identify human antigens to which a CD8$^+$ T cell repertoire existed in healthy individuals.

Most TEIPP-specific CD8$^+$ T cells reside in the naïve repertoire

Previous investigations in our mouse tumor model of TEIPP showed that TEIPP-specific T cells remain naïve, even in the presence of TAP-deficient tumor cells [15]. This was shown to be an advantage for their exploitability in therapeutic interventions [15]. To test this aspect for human TEIPP-specific T cells, we again enriched tetramer-positive CD8$^+$ T cells from PBMC for the five peptides p14, p29, p34, p35 and p55 that were frequently positive in our screen. Naïve CD8$^+$ T cells were directly separated from antigen-experienced CD8$^+$ T cells by flow cytometry sorting, based on differentiation markers CD62L and CD45RA at the cell surface (supplementary figure 2a). After this *ex vivo* sorting, the two populations were expanded by three rounds of *in vitro* stimulation and analyzed for the presence of tetramer-positive CD8$^+$ T cells (figure 3a-b). Importantly, T cells against p14, p34 and p35 were exclusively found in the sorted naïve population in all tested donors, indicating that these specificities had never encountered cognate antigen in these healthy individuals. In addition, T cells against p29 and p55 were found in the naïve subset of some donors while in other donors, these specificities were detected in the antigen-experienced repertoire (figure 3b). These data indicated that some TEIPP-specific CD8$^+$ T cells already had been

primed in a few healthy individuals, but that the majority of them reside in a naïve state. We speculated that this priming could have been triggered by bacterial species in the gut with antigens that show striking sequence similarity with peptide 29 and 55 (supplementary figure 2b). In summary, these data demonstrate a universal existence of naïve T cells with TEIPP specificity in healthy individuals.

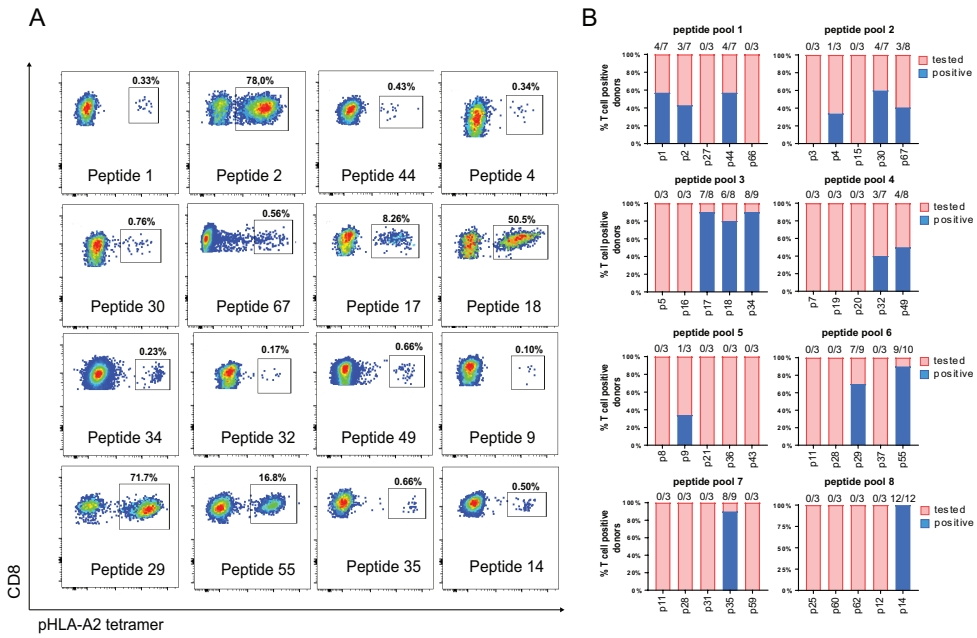

Figure 2: Detection of CD8⁺ T cells against TEIPP neoantigens in PBMC of healthy donors

PBMCs of healthy donors were screened with HLA-A*02:01 tetramers to identify whether a T cell repertoire is present for TEIPP neoantigens. HLA-A*02:01 tetramers folded with the selected 40 TEIPP neoantigen candidates were arranged in eight pools based on predicted peptide binding. (**A**) TEIPP enriched T cell pools were analyzed by flow cytometry (n=3). Representative dot plots of TEIPP neoantigen-specific CD8⁺ T cells are shown. (**B**) PBMCs of additional healthy donors were tested to validate the presence of a TEIPP T cell repertoire. All 40 TEIPP neoantigen-candidates were tested in at least three different donors. Shown are data of all tested donors. Each bar represents one TEIPP neoantigen-candidate. In blue the percentage of T cell positive donors based on flow cytometry analysis. Numbers above each bar indicate the fraction of positive donors out of total tested.

Functional avidity of clonal CD8⁺ T cell cultures

To functionally study TEIPP-specific CD8⁺ T cells, we generated clonal cultures against the five TEIPP peptides p14, p29, p34, p35, and p55. Four of these peptides were derived from N-terminal signal sequences of proteins and one was derived from a C-terminal 'tail peptide' (supplemental figure 2c). We evaluated the binding affinity and stability of these five peptides to HLA-A*02:01, since these determinants are critically involved in immunogenicity for T cells [32,33]. Four of the five peptides displayed an intermediate affinity and formed complexes with HLA-A*02:01 for at least four hours, however, p29 surprisingly failed to show binding in these cellular assays (supplementary figure 2d-e). Multiple T cell clones were generated using an antigen-independent expansion protocol of tetramer-positive CD8⁺ T cells after single cell sorting. Since the functional avidity correlates with high affinity TCRs and thus for *in vivo* efficacy [34-37], we assessed the peptide concentrations resulting in half maximum cytokine response (EC50) of the several TEIPP-specific T cell clones when exposed to antigen-presenting cells pulsed with titrated concentrations of cognate peptide (figure 3c). All isolated T cell clones exhibited a functional avidity between 0.4-66 nM, with the highest avidity for clones recognizing p34 and p55. The other clones, like those against p14, were considered to display moderate avidity. Of note, all clones with the same peptide specificity used different TCRβ V-segments, pointing at their independent origin and the availability of a broad repertoire (supplementary figure 2f). These results demonstrated that the broad repertoire of TEIPP-specific T cells in healthy individuals exhibits a usual functional avidity for their cognate peptide and is competent to respond upon antigen encounter.

CD8⁺ T cells against p14 recognize TAP-deficient tumors across diverse histological origin

In search for TEIPP antigens on immune-escaped cancers, we selected the p14 peptide-epitope with sequence FLGPWPAAS from the ubiquitously expressed LRPAP1 protein (from now on called $LRPAP1_{21-30}$) for in depth examination (Table I). First, we confirmed specificity for the $LRPAP1_{21-30}$ epitope for T cell clone 1A8 by testing different peptide length variants of the LRPAP1 signal peptide (supplementary figure 3a). Although unconventional, this examination confirmed the serine amino acid as C-terminus for this HLA-A*02:01 allele. Next, LRPAP1 gene expression data was collected from the TCGA database for different tumor types, revealing that its expression is ubiquitous with exceptionally high expression levels in skin melanomas (figure 4a). We therefore selected the HLA-A*02:01 positive skin melanoma cell line '518A2' and confirmed the expression of the LRPAP1 gene (figure 4b, supplementary figure 3b). For this cell line an TAP1 knock-out variant, a CRISPR/CAS9 control TAP1-WT variant, and an TAP1/antigen double knock-out variant were generated by CRISPR/CAS9 technology and these gene edited variants were tested for recognition by the

Table I. Overview TEIPP neoantigen candidates

#	Gene Name	Peptide[1] Sequence	Accession[2] Number	HLA-A2[3] Affinity (IC50)	Expression[4]			T cell Repertoire
					Tissue[5]	Normal	Cancer	
Ubiquitous TEIPP								
p1	ERGIC3	FLSELQYYL	Q9Y282	2	All	++	++	4/7
p4	TTYH3	ALFSFVTAL	Q9C0H2	10	All	+	+	1/3
p9	IGJ	VLAVFIKAV	P01591	52	All	++	++	1/3
p14	LRPAP1	FLGPWPAAS	D6REW6	353	All	++	++	14/14
p29	ARSA	LLALAAGLAV	P15289	79	All	++	++	9/10
p44	EMILIN2	FLYPFLSHL	Q9BXX0	4	All	+	++	4/7
p49	H2AFV	ILEYLTAEV	E5RJU1	30	All	++	++	6/9
p67	SEP15	LSEKLERI	O60613	15	All	+	+	4/8
Tissue Specific TEIPP								
p2	IL12A	VLLDHLSLA	P29459	7	Mixed	+	+	3/7
p17	HPR	LLWGRQLFA	P00739	24	Liver	+++	+	6/7
p18	FSTL4	TLLGASLPA	Q6MZW2	27	Mixed	+	+++	5/7
p30	IFI30	LLLDVPTAAV	M0QZG3	10	Mixed	++	++	5/8
p32	CD79B	LLLSAEPVPA	P40259	41	Lymphoid	+	++	3/7
p34	PCDHGA6	LTLLGTLWGA	Q9Y5G7	24	Mixed	+/-	+/-	8/8
p35	C20orf141	SVLWLGALGL	Q9NUB4	161	Testis	+	+	16/16
p55	APCS	VIIKPLVWV	P02743	113	Liver	+++	+++	9/10

[1.] Peptide sequence based on predicted signal peptide cleavage site
[2.] Accession number uniprot.org
[3.] Predicted peptide affinity binding in HLA-A2:01
[4.] Protein expression scores based on data proteinatlas.org
[5.] Protein expression based on TCGA database score

LRPAP1$_{21\text{-}30}$-specific CD8$^+$ T cell clone 1A8 (figure 4b, supplementary figure 3c-d). Surface display of HLA-A*02:01 decreased after knocking out the gene for the peptide transporter TAP1 (figure 4c). The LRPAP1$_{21\text{-}30}$-specific CD8$^+$ T cell clone selectively recognized the TAP1-deficient variant of 518A2. This suggested that the LRPAP1$_{21\text{-}30}$ signal peptide was only presented by the TAP-deficient tumor variant, despite equal expression of the *LRPAP1* gene and lower HLA-A*02:01 levels on these cells (figure 4d). Furthermore, selective knockout of the epitope ('LRPAP1$_{21\text{-}30}$ Ag-KO') resulted in complete abrogation of T cell recognition (figure 4d). To control for artificial CRISPR/CAS9-induced immunogenicity, we included a previously established T cell clone (HSS1 PRAME) that recognizes the TAP-dependent

PRAME (SLLQHLIGL) tumor antigen. This $PRAME_{425-433}$-specific $CD8^+$ T cells only recognized 518A2 WT cells whereas it completely failed to respond towards the TAP KO variant. In contrast, $LRPAP1_{21-30}$-specific T cells displayed clear preference for the TAP KO variant (figure 4e). Collectively, these data confirmed that the applied tetramer-based selection approach allows the isolation of functional $CD8^+$ T cells with a bona fide specificity for the antigen from which the TEIPP was derived. Moreover, these data excluded potential cross-reactivity of T cell clone 1A8 against other peptides presented by the 518A2 melanoma cells. Finally, antibodies against HLA-I molecules were able to block the tumor recognition by T cells, demonstrating dependency on peptide/HLA-I (figure 4f).

The ubiquitous expression of the *LRPAP1* gene in diverse tumor types prompted us to test T cell recognition of other HLA-A*02:01 positive melanomas and tumors of other histological origin, including renal cell carcinoma and lymphoma. The panel of T1 and T2 lymphoma cells are known for their characterized genomic TAP status (supplementary figure 3e) [38,39]. We confirmed equal *LRPAP1* gene expression by quantitative PCR (supplementary figure 3f) and examined recognition by multiple $LRPAP1_{21-30}$-specific T cell clones (figure 4g). All tested $CD8^+$ T cell clones selectively recognized the TAP-deficient T2 cells, again displaying a typical TEIPP specificity.

Next, a panel of HLA-A*02:01 positive TAP-deficient melanomas and renal cell carcinomas were generated by genetically disrupting the *TAP1* gene. Tumor cell mRNA levels of the *LRPAP1* gene were again comparable as quantified by PCR (supplementary figure 3g). Flow cytometry analysis revealed that HLA-A*02:01 levels varied between the lines, but that these decreased after *TAP1* gene knockout (figure 4h). As observed for the 518A2 melanoma and the T2 lymphoma, multiple $LRPAP1_{21-30}$-specific T cell clones exhibited a preferential recognition of the TAP1-deficient tumor lines (figure 4i). Interestingly, some parental tumors were already recognized even before silencing the *TAP1* gene (e.g. melanoma 93.04), implying that the endogenous *TAP1* levels were already lower expressed to allow presentation of the $LRPAP1_{21-30}$ antigen. Indeed, quantitative PCR confirmed low *TAP1* gene expression in the melanoma 93.04 (supplementary figure 3h). In line with this, complete abolishment of the *TAP1* gene in tumor line 93.04 did not result in much improved T cell recognition (figure 4i). To further corroborate the shared character across multiple tumor types, we also tested T cell recognition of our 1A8 clone against two colon carcinomas (supplementary figure 3i-j). Interestingly, we observed specific T cell responses towards the TAP KO variants of these two colon carcinoma cell lines (supplementary figure 3k). Overall, these data clearly demonstrated that the $LRPAP1_{21-30}$ TEIPP epitope is universally presented in HLA-A*02:01 by cancers of diverse histology when the peptide transporter TAP is not functional. TEIPP specific $CD8^+$ T cells specific for this TEIPP antigen enables targeting of this shared, nonmutated peptide on immune-escaped HLA-I^{low} cancers.

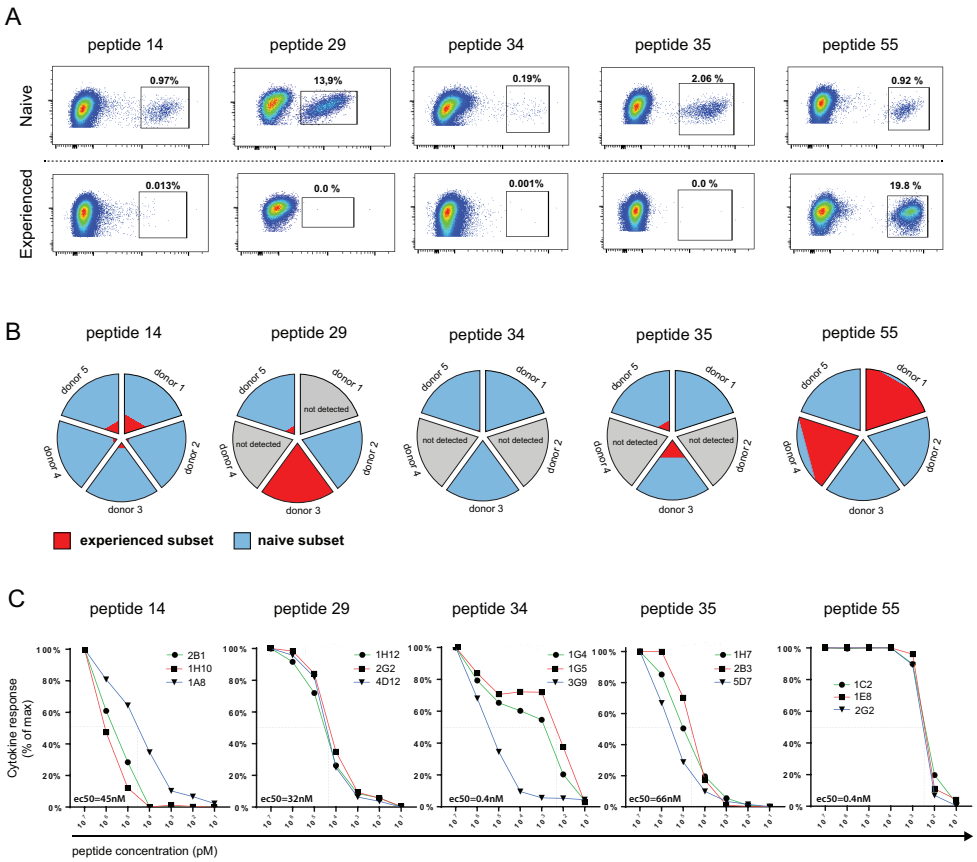

Figure 3: Most TEIPP-specific CD8⁺ T cells reside in the naïve repertoire

The status and functional avidity of TEIPP specific T cells peptide-candidates p14, p29, p34, p35, and p55 were examined. CD8⁺ T cells to these peptides were most abundantly detected in PBMCs of healthy donors. (**A**) Representative dot plots of pHLA-A*02:01 tetramer stained CD8+ T cells cultured from either the naïve subset or the experienced subset. Percentages represent pHLA-A*02:01 tetramer positive cells out of total CD8⁺ T cells. (**B**) Pie-charts for each of the TEIPP neoantigen-candidates. Five donors were tested and each slice represents one donor. Relative percentage of naïve cells (*blue)* and percentage of experienced cells (*red)* is calculated out of total pHLA-A*02:01 tetramer positive CD8⁺ cells. (**C**) T cell clones against these peptides were generated by single cell sorting on HLA-A*02:01 tetramer-positive cells and subsequent expansion. Functional T cell avidity was examined by measuring cytokine production of activated T cells recognizing TEIPP peptide pulsed HLA-A*02:01 positive T2 cells with different concentrations of peptide. EC50 was determined by calculating the peptide concentration (nM) corresponding to the 50% cytokine production of the maximum response (n=3). Individual clones were tested at least twice.

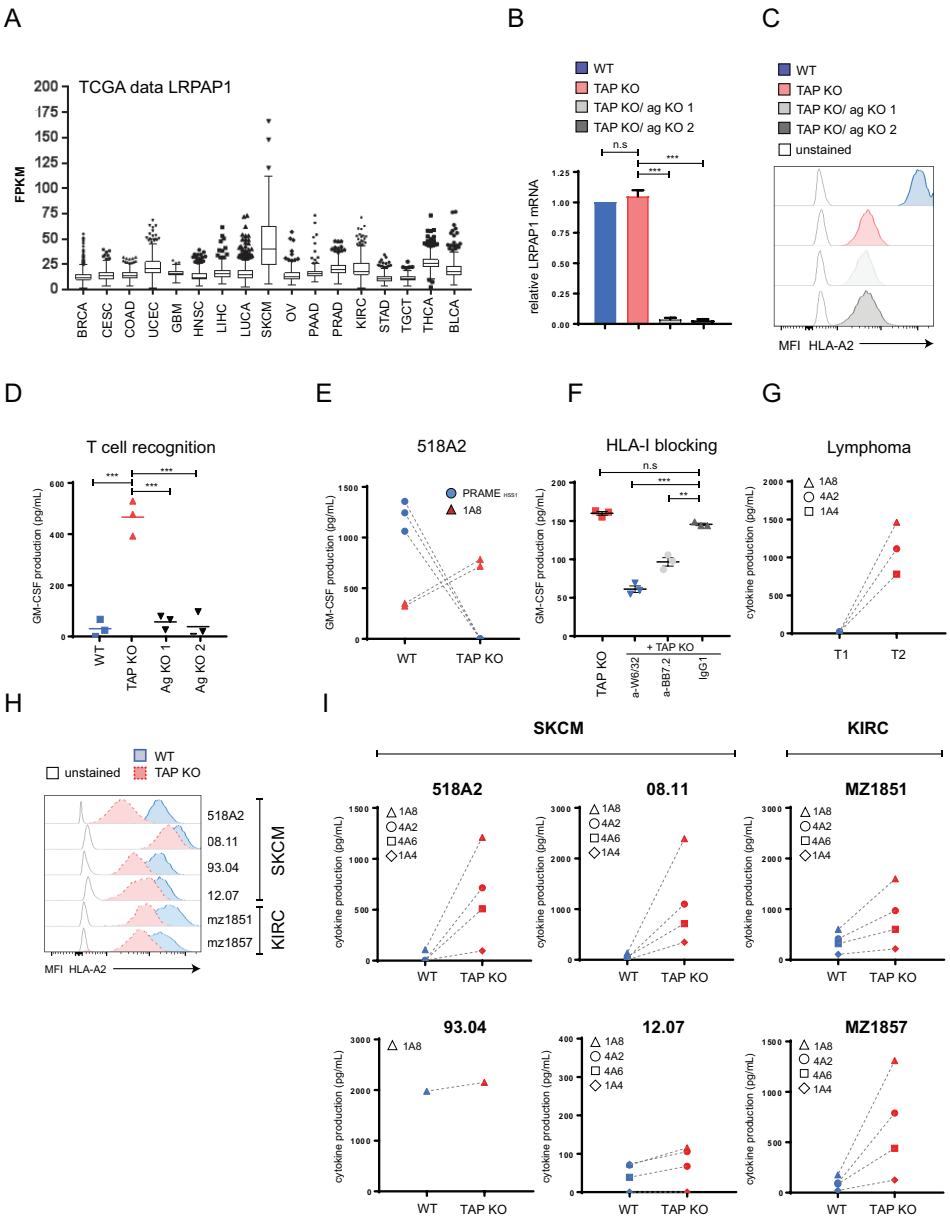
A
TCGA data LRPAP1
FPKM
BRCA
CESC
COAD
UCEC
GBM
HNSC
LIHC
LUCA
SKCM
OV
PAAD
PRAD
KIRC
STAD
TGCT
THCA
BLCA
B
WT
TAP KO
TAP KO/ ag KO 1
TAP KO/ ag KO 2
n.s
relative LRPAP1 mRNA
C
WT
TAP KO
TAP KO/ ag KO 1
TAP KO/ ag KO 2
unstained
MFI HLA-A2
D
T cell recognition
GM-CSF production (pg/mL)
WT
TAP KO
Ag KO 1
Ag KO 2
E
518A2
PRAME
1A8
GM-CSF production (pg/mL)
WT
TAP KO
F
HLA-I blocking
n.s
GM-CSF production (pg/mL)
TAP KO
+ TAP KO
a-W6/32
a-BB7.2
IgG1
G
Lymphoma
1A8
4A2
1A4
cytokine production (pg/mL)
T1
T2
H
WT
TAP KO
unstained
518A2
08.11
93.04
12.07
mz1851
mz1857
SKCM
KIRC
MFI HLA-A2
I
SKCM
KIRC
518A2
08.11
MZ1851
93.04
12.07
MZ1857
1A8
4A2
4A6
1A4
cytokine production (pg/mL)
WT
TAP KO

Figure 4: CD8⁺ T cells against p14 recognize TAP-deficient tumors of different histological origin

T cell clones were tested for their specificity to selectively recognize the $LRPAP1_{21-30}$ TEIPP epitope presented on TAP-impaired tumors. (**A**) Whisker plots of LRPAP1 gene expression in human cancers (data collected from TCGA database). (**B**) The TAP1 gene in the melanoma 518A2 was knocked out (TAP KO) using CRISPR/CAS9. In addition, the $LRPAP1_{21-30}$ epitope was knocked out in these cells (ag KO). mRNA expression of LRPAP1 was examined by qPCR. Data are shown as mean ± SD of triplicates. Significance testing: unpaired t test, n.s., not significant; ***, p<0.001 (n=3). (**C**) HLA-A*02:01 surface expression on 518A2 melanoma variants, measured by flow cytometry. Plots are representative of three independent experiments. (**D**) GM-CSF production of T cell clone 1A8 upon 518A2 TAP KO recognition. When $LRPAP1_{21-30}$ epitope was knocked out (ag-KO), recognition by the T cells were abolished. Representative data of three independent experiments is shown. Each dot represents a technical replicate. Significance testing: unpaired t test, ***, p<0.001. **(E)** To control for artificial CRISPR/CAS9 mediated immunogenicity, we co-cultured T cell clones specific for $LRPAP1_{21-30}$ (TAP-independent epitope) or $PRAME_{425-433}$ (TAP-dependent epitope) together with the 518A2 melanoma (WT vs TAP KO). GM-CSF cytokine response was measured. Each dot represents one independent experiment with technical triplicates. (**F**) HLA-dependency was tested using HLA-ABC or HLA-A*02:01 blocking antibodies. Representative data of two independent experiments is shown. Each dot represents a technical replicate. Significance testing: unpaired t test, n.s., not significant, **, p<0.01; ***, p<0.001. (**G**) TEIPP T cell specificity was determined by co-culturing three different T cell clones together with TAP-proficient T1 cells and TAP-deficient T2 lymphoma cells. Cytokine responses were measured to detect T cell recognition. Representative data of three independent experiments with technical triplicates is shown. (**H**) HLA-A*02:01 surface expression of the TAP-impaired tumor panels as measured by flow cytometry (SKCM: melanoma; KIRC: renal carcinoma). Representative data of three independent experiments is shown. (**I**) Cytokine production of indicated T cell clones upon antigen recognition of four melanomas and two renal carcinomas. Each dot represents one T cell clone specific for the $LRPAP1_{21-30}$ epitope. Representative data of three independent experiments with technical triplicates is shown.

Targeting TEIPP antigens appear safe despite ubiquitous expression of their proteins in healthy cells

The fact that human TEIPP antigens derive from ubiquitously expressed nonmutated proteins may raise concerns for autoimmune pathology. Indeed, the LRPAP1 protein is clearly expressed in several critical organs of our body, as revealed by tissue slide staining images available from proteinatlas.org (figure 5a, supplementary figure 4a)[40]. Therefore, two primary melanocyte cultures and two immortalized kidney cell lines were tested for $CD8^+$ T cell recognition. These non-transformed cells contained similar high levels of LRPAP1 transcripts as the 518A2 tumor (figure 5b) and displayed sufficient levels of HLA-A*02:01 at their cell surface (figure 5c). Despite these optimal conditions, $LRPAP1_{21-30}$-specific T cells did not respond to these healthy cells (figure 5d). Exogenous loading of synthetic LRPAP1 peptide to the cells, however, did lead to LRPAP1-specific T cell response, suggesting that healthy cells were capable of presenting peptides (figure 5e). These data confirmed a crucial role for low TAP function for the presentation of TEIPP antigens and suggested that TEIPP targeting might be considered a safe therapy, even though these proteins are present in healthy tissues as well.

In summary, our data reveals an array of novel nonmutated tumor antigens displayed by tumors with (partial) TAP deficiency (Table I). Some of these are tissue restricted, but others, like the LRPAP1 signal peptide, are ubiquitously expressed and represent universal HLA-presented tumor antigens on cancers with impaired antigen processing.

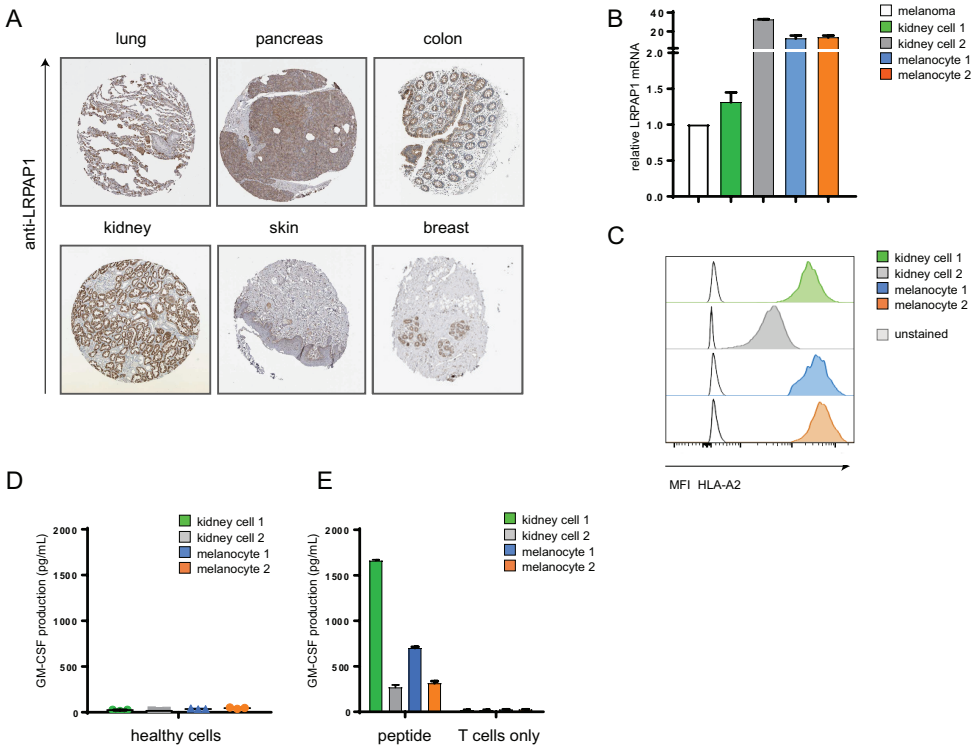

Figure 5: Targeting TEIPP antigens is safe despite ubiquitous expression of their proteins in healthy cells

To assess the safety of targeting nonmutated TEIPP neoantigens we examined the T cell recognition of healthy cells. (**A**) Histological tissue stainings for LRPAP1 were collected from an online accessible database (www.proteinatlas.org). Positive protein detection was observed in various healthy organs. (**B**) *LRPAP1* mRNA levels were determined of two primary melanocyte cultures and two non-transformed kidney epithelial cell lines by qPCR. Data are shown as mean ± SD from one out of two experiments. (**C**) Surface HLA-A*02:01 expression of the healthy cells was determined by flow cytometry. Representative data of three independent experiments is shown. (**D**) No cytokine responses were detected when T cells specific for $LRPAP1_{21-30}$ were co-cultured with these healthy cells. Representative triplicate data of two independent experiments are shown. (**E**) To assess the ability of the healthy cells to present the epitope in HLA-A*02:01, peptide was exogenously loaded. $LRPAP1_{21-30}$ specific T cell clone 1A8 was co-cultured with peptide pulsed healthy cells and GM-CSF cytokine production was measured. Representative triplicate data of two independent experiments are shown.

Discussion

We developed a screening approach to identify human antigens belonging to the novel category of non-mutated neoantigens of 'self' origin, called TEIPP. Our screen yielded 65 potential TEIPP candidates, which are exclusively present in the peptidome of cancer cells. Analysis of the 40 HLA-A*02:01 binding TEIPP candidates revealed a consistent $CD8^+$ T cell repertoire to 16 of these 40 peptides. Additional analyses demonstrated that these $CD8^+$ T cells were present in the naïve pool for five peptide-candidates and that they were not affected by central or peripheral tolerance. Monoclonal T cell cultures against the TEIPP epitope $LRPAP1_{21\text{-}30}$ selectively recognized TAP1-deficient cancers from different histological origins, including lymphoma, melanoma, colon carcinoma, and renal cell carcinoma, whereas TAP-proficient primary cells were spared from T cell recognition. This emphasizes the attractiveness of targeting TEIPP neoantigens on HLA-I^{low} cancers, namely for its shared character on those tumor cells. Thus far we focused on HLA-A*02:01 binding TEIPP peptides, but our screen also predicted a broad array of antigens presented by other HLA types. Furthermore, we realize that this proof-of-concept approach is far from complete. Most likely, many more undiscovered pathways enable the presentation of TAP-independently processed TEIPP neoantigens.

We observed that knocking out the *TAP1* gene rendered all tested cancer cell lines vulnerable for TEIPP-specific T cells. Importantly, TEIPP-specific T cells exhibited moderate to high recognition of some wild-type skin melanomas and renal cell carcinomas (e.g. 93.04, mz1257), and CRISPR/CAS9 mediated knockout of the *TAP1* gene led to only modest improvement of cancer cell recognition. In other cancer lines (e.g. melanoma 518A2, 08.11), minimal T cell responses were detected to wild-type cancer cells and knockdown of TAP1 was necessary to induce strong T cell recognition. These data suggested that some cancer cell lines already down modulated TAP1 gene expression in such degree that was already sufficient for the presentation of TEIPP neoantigens. Although only 1-2% of melanomas have deleterious mutations in TAP1 or TAP2, a high frequency of metastatic melanomas display low TAP1 expression due to epigenetic silencing [5,7]. At this moment, we have not determined how low TAP1 function needs to be for TEIPP neoantigens to be presented on the cell surface of cancer cells. The exact mechanisms of selective TEIPP neoantigen presentation on antigen processing defective cells are still not completely known. Our previous experiments in mouse models suggested a competition between peptide antigens in the endoplasmic reticulum[37,41]. The peptide loading complex (PLC) is a multisubunit membrane complex orchestrating the loading and editing of peptides in HLA-I molecules, facilitated by the TAP1/TAP2 channel, and thereby responsible for the translocation of peptides from the cytosol into the PLC complex[42]. The TAP peptide transporter is incorporated in this

efficient peptide loading complex, in close proximity to HLA-I molecules, which could explain why peptides processed through different mechanisms, independent of TAP, will not have the chance to bind in HLA-I molecules. Besides TAP levels, the amount of available antigenic protein also needs to be taken into account. Interestingly, massive overexpression of a TEIPP antigen makes it possible to present its TEIPP peptide in the cell surface even in TAP-proficient cells[41]. We theorize that these two factors govern the efficiency of TEIPP neoantigen presentation. Low TAP function allows for low antigen expression, whereas moderate TAP function needs higher amounts of antigen expression[17,41]. Of utmost importance is that TAP function in healthy cells of our organs is high enough to prevent recognition by TEIPP-specific T cells[14,15].

The presence of a TEIPP T cell repertoire in healthy donors indicates that no negative selection has occurred in the thymus, even though gene expression in the thymus was observed for most of the TEIPP neoantigen-candidates (supplementary figure 4b). During T cell education in the thymus TEIPP-specific T cells are positively selected for low affinity interaction with peptide/MHC in the cortex of the thymus. To prevent autoimmune responses, negative selection of T cells in the medulla of the thymus is essential to delete self-reactive T cells. This strengthens the hypothesis that TAP-proficient medullary thymic epithelial cells (mTECs) might express the target proteins but do not present TEIPP antigens by their HLA-I and thus TEIPP T cells will undergo normal thymic selection. Indeed, TEIPP-specific T cells are deleted from the repertoire of TAP-deficient mice [14]. Moreover, most of the evaluated TEIPP-specific T cells were only found in the naïve pool in the circulation and have not encountered antigen yet, signifying that TAP-proficient healthy cells did not trigger TEIPP-specific immunity. Also, we presume this observation hold true in cancer patients, since tumor cells are no real APCs in an immune suppressive environment. Ex-vivo T cell activation or synthetic long peptide vaccination strategies are needed for proper TEIPP directed anti-tumor responses. These data mirror earlier observations in our mouse model for TEIPP [15]. Some viruses are also known to down regulate TAP (e.g. EBV, CMV). Yet, we find most TEIPP-specific T cells in the naïve repertoire. An explanation for this could be that viruses also manipulate other pathways () leading to immuno suppressive effect and no T cell activation accordingly. Noteworthy, in some donors we observed that T cells against p29 and p55 were derived from the antigen-experienced pool. We speculate that these TEIPP specificities had been triggered by cross-reactivity to microbiota-derived epitopes leaked from the gut, which can occur after the use of antibiotics or other intestinal injury [43,44]. Since the tested healthy donors did not suffer from severe autoimmune reactivity, even antigen-experienced TEIPP-specific T cells apparently do not target healthy TAP-proficient tissues. The safety of TEIPP-targeting therapies was thoroughly evaluated in mouse tumor models [14,15,45-47]. Vaccine-induced TEIPP-specific T cells via synthetic peptides or dendritic

cells, or adoptive transfer of TEIPP-specific T cells all reduced outgrowth of TAP-deficient tumors without any sign of autoimmune reactivity.

TEIPP neoantigens are selectively presented in cancer cells with deficient function of MHC-I processing machinery. Therefore, we anticipate a complementary role for these antigens to those of other categories, like patient-specific mutanome peptides or cancer-testis antigens. A combination of those might prevent immune-escape via shutdown of HLA-I expression due to defects in the antigen processing machinery. A great asset of TEIPP antigens is their non-mutated status and the fact that the tumor antigens are broadly shared across many cancer types. A few validated TEIPP antigens or gene transfer of their cognate cloned T cell receptors might be sufficient for increased efficacy of immunotherapy through prevention of tumor escape. Future investigations need to reveal safety and applicability of vaccination-based strategies and TCR-based gene transfer approaches for TEIPP. Together, we propose that TEIPP neoantigens are an interesting way to re-establish anti-tumor responses in human immune-escaped cancers.

Material and methods

Study design

The aim of this study was to test a systematic hybrid forward-reversed immunology approach to identify TEIPP specific T cells and their cognate antigen (Table I). For this, we collected the whole human proteome dataset from uniprot.org (ID: 9606, Release: 2014_06). For predictions of the N-terminal "signal" cleavage location and the topology prediction for C-terminal "tail" peptides the web-based topology algorithm Phobius was used (*htpp://www.phobius.edu/)*. For N-terminal peptide candidates, proteins with a predicted signal peptide probability of >0.5 were included. For C-terminal peptide candidates, proteins with a predicted C-terminal "tail" located in the ER were included. Peptide binding affinity to HLA-I molecules were predicted using MHCnet4.0 (*http://www.cbs.dtu.dk/*). Peptides with a predicted binding affinity <500 nM were included. We used the peptidome elution library (release 2014_10) of the Tübingen group (Department of Immunology, Tübingen) to select for biologically processed peptides. Next, in vitro analysis was performed on forty HLA-A*02:01 TEIPP candidates using healthy donor PBMC. In depth analysis was performed on five TEIPP candidates. To guarantee statistical power, we performed all experiments on at least three different PBMC batches isolated from different donors.

Tumor cell lines

Human tumor cell lines were obtained through ATCC or derived from patient surgery material. The clinical protocol was approved by the Medical Ethics Committee of the LUMC and

conducted in accordance with the declaration of Helsinki. All tumor cell lines were cultured at 37°C, 5% CO_2, in DMEM medium (Invitrogen, Carlsbad, CA) containing 8% heat-inactivated FCS, 100 U/mL penicillin, 100 µg/mL streptomycin (Life Technologies, Rockville, MD) and supplemented with 2 mM glutamine (Invitrogen).

Generation of TEIPP specific T-cell clones

Buffy coats from healthy donors were obtained from Sanquin (Sanquin blood facility). Informed consent was given in writing by all participants. PBMC's were isolated using a ficoll gradient (density 1.077 g/mL). Approximately $500x10^6$ PBMC's were incubated with PE-pHLA-A*02:01 tetramers for 30 min at 4°C. Anti-PE magnetic beads (MACS) were used to pull out pHLA-A*02:01 tetramer positive cells over a MACS LS column as instructed by the manufacturer (Miltenyi Biotech). T cells were cultured in complete IMDM containing 8% human serum (Sanquin blood facility), and 100 U/mL IL-2 (Proleukine, Novartis). Bulk T cells were stimulated every two weeks with a mixture of T cells ($1x10^6$), 10 µM synthetic peptide, irradiated PBMCs ($1x10^6$ cells, 80Gy) and EBV-JY ($1x10^5$ cells, 100Gy) in complete T cell culture medium supplemented with 100 U/mL IL-2 in 24-well plates (Costar). Culture medium was replenished every 2 to 3 days with fresh complete T cell medium. After two rounds of specific stimulation, the polyclonal T cell bulk was incubated with PE labeled tetramers and single cell sorted using flow cytometry to obtain monoclonal T cells. After monoclonal cell sorting, T cell clones were stimulated with a phytohemagglutinin (PHA) mixture (complete T cell medium supplemented with 800 ng/mL PHA (Murex Biotech) and 100 U/mL IL-2) together with irradiated PBMCs ($50x10^5$ cells, 80Gy) and EBV-JY cells ($10x10^4$ cells, 100Gy) per 96-well.

Generation of pHLA-A*02:01 tetramers

Ultra-pure peptides were synthesized by JPT peptide technology. Recombinant HLA-A*02:01 and human β2m proteins were in-house synthesized in *Escherichia coli* [48,49]. Biotinylated HLA-A*02:01 molecules were produced containing an ultraviolet (UV)-sensitive peptide to enable easy transfer of specific peptide, as previously described [50]. In brief, HLA-A*02:01 complexes were purified by gel filtration using Fast protein liquid chromatography (FPLC). pHLA-A*02:01 complexes were exposed to UV light to facilitate peptide exchange resulting in peptide specific monomers. pHLA-A*02:01 tetramers were formed by coupling biotinylated pHLA-A*02:01 monomers with streptavidin-coupled R-phycoerythrin conjugate (PE, ThermoFisher). Tetramers were stored at -80°C for long-term storage or 4°C for short-term storage.

Co-culture T cell reactivity assay

Dependent on the T cell clone, GM-CSF (T cell clone 1A8 and PRAME), or IFN-γ (all other tested T cell clones) ELISA assays (GM-CSF, MabTech, IFN-γ, Pelikine) were used to measure the cytokine production of activated T cells. ELISA plates were coated with human IFN-γ or GM-CSF primary antibody overnight at 4°C. T cell conditioned medium was collected incubated in the pre-coated ELISA plates for two hours at room temperature. Next, ELISA plates were washed with PBS-T followed by incubation with the HRP conjugated secondary antibody for one hour. ELISA plates were developed with TMB (3,3,5,5-tetramethyl-benzidine liquid substrate supersensitive, for ELISA; Sigma-Aldrich) and measured at 450 nm using a plate reader (Spectramax id3, Molecular Devices). Lower cut-off values for cytokine production were calculated as medium values plus three times the standard deviation. Values below this threshold were considered negative. All plotted values were within the upper and lower detection limits of the ELISAs.

Affinity and stability assay

Peptide affinity and stability were determined as previously described [33,51]. In brief, HLA-A*02:01^{+} T2 cells were pulsed with increasing concentrations of peptide (1 uM-100 uM) in serum free RPMI culture medium for 24 hours at 37°C. For MHC:peptide affinity, the maximum HLA-A*02:01 expression was measured by flow cytometry to calculate the EC50 concentration. For MHC:peptide stability, HLA-A*02:01 positive T2 cells were pulsed with 100 uM peptide for 24 hours at 37°C. Maximum HLA-A*02:01 expression was determined and followed over time to calculate the $T_{1/2}$ value.

Generation of gene knockouts in tumor cells using CRISPR-CAS9

sgRNAs were designed to target exon 1 of the human TAP1 gene (sgTAP1: GCTGCTACTTCTCGCCGACT) or the $LRPAP1_{21-30}$ epitope located in exon 1 ($LRPAP1_{21-30}$:AGGGTCAGGTCGTTTCTGCG). The sgRNA target sequence was cloned into the lentiCRISPR v2 vector [52]. Virus particles were generated by co-transfecting sgRNA/CAS9 containing plasmid together with PAX2/pMD2.G packaging vectors into HEK293T cells using lipofectamine 2000 (ThermoFisher). Tumor cells were incubated with medium containing the virus particles for 24 hours and transduced tumor cells were selected with 1-5 ug/mL puromycin (Gibco). TAP1 knockout-efficiency was analyzed by measuring surface HLA-ABC (w6/32, Biolegend) expression using flow cytometry. Polyclonal TAP knockout cell lines were generated by FACS sorting the HLA-I^{low} cell population. CRISPR/CAS9 TAP-WT control cells were generated by FACS sorting the HLA-I^{high} cell population of the polyclonal bulk. TAP1 expression was verified by Western-Blot using anti-TAP1 antibodies (Cell Signaling).

Western Blot

Proteins from cell cultures were extracted in lysis buffer (RIPA, Cell Signaling), and protein concentrations were assessed using the Bradford Protein Assay Kit (Thermo Fisher). Protein samples were separated on a 4-12% SDS–polyacrylamide gel electrophoresis gel and transferred onto nitrocellulose membranes using semi-dry transfer (BioRad). To prevent a-specific binding, membranes were blocked with 5% milk in TBS-T for one hour at room temperature. Antibodies used: anti-TAP1 (dilution 1:1000, 4°C¸ Cell Signaling), anti- β-actin (dilution 1:1000, 4°C, Cell Signaling), HRP linked mouse anti-Rabbit IgG (dilution 1:5000, RT, Cell Signaling).

Flow cytometry analysis

CD3 (SK7), CD4 (SK3), CD8 (SK1), CD45RO (UCHL1), HLA-A*02:01 (bb7.2)(BD Biosciences), and HLA-ABC (MCA81A), CD45RA (HI100), CD62L (DREG-56) (Biolegend) anti-human mAbs were used for flow cytometry analysis. Cells were incubated with mAbs for 30min at 4°C and washed three times. Unstained cells were used as negative controls. The Vβ Repertoire analysis kit was used to determine the TCR Vβ of the different monoclonal T cells (Beckman Coulter). For T cell specificity analysis, we incubated T cells with pHLA-A*02:01 tetramers for 30min at RT and washed 3 times. T cells were considered tetramer positive when MFI was at least 10^2 times higher than unstained control. Cells were measured using a LSR-II flow cytometer (BD biosciences) and analyzed using Flowjo software version 10 (Tree Star).

mRNA isolation, cDNA synthesis, and qPCR analysis

Cell pellets were washed twice with PBS and snapfrozen in liquid nitrogen. RNA was isolated using the RNAeasy kit (Qiagen), according to manufactures protocol. cDNA was synthesized using the High capacity RNA-to-cDNA kit (Applied Biosystems). Quantitative PCR was done using SybrGreen supermix (Bio-Rad). For qPCR analysis we used the following primers. GAPDH_f: GTGCTGAGTATGTCGTGGAGTCTAC; GAPDH_r: GGCGGAGATGATGACCCTTTTGG; TAP1_f: CTTGCAGGGAGAGGTGTTTG; TAP1_r: GAGCATGATCCCCAAGAGAC; LRPAP1_f: GACCGAAGAAATCCACGAGA; LRPAP1_r: AGGTCCCACAGGTCAATCAC.

Statistical analysis

All data are presented as means and SD. Statistical analysis was done using a paired Student's t test (two-tailed) to determine the statistical significance of the differences. A minimum of three technical replicates were used in all experiments, and were repeated at least two times.

Online supplemental material:

Table SI. shows an overview of the number of histological tissue samples and cancer samples that are used to create the peptide elution database. In Fig. S1, we plotted the results of the predicted TEIPP candidate peptide binding in HLA-I. Fig. S2 shows the characterization of TEIPP T cells, sequence, binding affinity and stability of the TEIPP antigens, and homology with bacterial peptides. In Fig. S3, mRNA and protein expression analysis of LRPAP1 and TAP1 on the tumor panel, and functional T cell assays are shown to support the findings in figure 4 in the main text. Fig. S4 illustrates the protein expression analysis of TEIPP candidates in healthy and cancer tissue.

Author contributions:

T.H. and S.H.B. designed the project. K.A.M. and L.B. performed and designed all experiments. M.G.K., and K.A.M. synthesized the tetramers. E.V. provided all cancer cell lines. K.A.M. and T.H. wrote the manuscript. D.K. performed peptide matching analysis. HG.R. and S.S. shared their peptidome databases. K.A.M., T.H. and S.H.B. interpreted data. S.H.B., HG.R., S.S., and M.H.M.H. reviewed and edited the manuscript.

Acknowledgments:

We thank the peptide synthesis core facility and the flow cytometry core facility for their contribution to this project. Funding: This work was supported by the Dutch Cancer Foundation (2013-6142 for K.A.M.). Data and materials availability: Peptide elution database was made available by the Department of Immunology, Tübingen. The authors declare no competing financial interests.

References and Notes:

1 Robbins, P. F. *et al.* Mining exomic sequencing data to identify mutated antigens recognized by adoptively transferred tumor-reactive T cells. *Nat Med* **19**, 747-752, doi:10.1038/nm.3161 (2013).

2 Schumacher, T. N. & Schreiber, R. D. Neoantigens in cancer immunotherapy. *Science* **348**, 69-74, doi:10.1126/science.aaa4971 (2015).

3 Lauss, M. *et al.* Mutational and putative neoantigen load predict clinical benefit of adoptive T cell therapy in melanoma. *Nat Commun* **8**, 1738, doi:10.1038/s41467-017-01460-0 (2017).

4 Snyder, A. *et al.* Genetic basis for clinical response to CTLA-4 blockade in melanoma. *N Engl J Med* **371**, 2189-2199, doi:10.1056/NEJMoa1406498 (2014).

5 Ritter, C. *et al.* Epigenetic priming restores the HLA class-I antigen processing machinery expression in Merkel cell carcinoma. *Sci Rep* **7**, 2290, doi:10.1038/s41598-017-02608-0 (2017).

6 Setiadi, A. F. *et al.* Epigenetic control of the immune escape mechanisms in malignant carcinomas. *Mol Cell Biol* **27**, 7886-7894, doi:10.1128/MCB.01547-07 (2007).

7 Garrido, F., Aptsiauri, N., Doorduijn, E. M., Garcia Lora, A. M. & van Hall, T. The urgent need to recover MHC class I in cancers for effective immunotherapy. *Curr Opin Immunol* **39**, 44-51, doi:10.1016/j.coi.2015.12.007 (2016).

8 Patel, S. J. *et al.* Identification of essential genes for cancer immunotherapy. *Nature* **548**, 537-542, doi:10.1038/nature23477 (2017).

9 Sucker, A. *et al.* Acquired IFNgamma resistance impairs anti-tumor immunity and gives rise to T-cell-resistant melanoma lesions. *Nat Commun* **8**, 15440, doi:10.1038/ncomms15440 (2017).

10 Gao, J. *et al.* Loss of IFN-gamma Pathway Genes in Tumor Cells as a Mechanism of Resistance to Anti-CTLA-4 Therapy. *Cell* **167**, 397-404 e399, doi:10.1016/j.cell.2016.08.069 (2016).

11 Shin, D. S. *et al.* Primary Resistance to PD-1 Blockade Mediated by JAK1/2 Mutations. *Cancer Discov* **7**, 188-201, doi:10.1158/2159-8290.CD-16-1223 (2017).

12 Zaretsky, J. M. *et al.* Mutations Associated with Acquired Resistance to PD-1 Blockade in Melanoma. *N Engl J Med* **375**, 819-829, doi:10.1056/NEJMoa1604958 (2016).

13 Marijt, K. A., Doorduijn, E. M. & van Hall, T. TEIPP antigens for T-cell based immunotherapy of immune-edited HLA class I(low) cancers. *Mol Immunol*, doi:10.1016/j.molimm.2018.03.029 (2018).

14 Doorduijn, E. M. *et al.* TAP-independent self-peptides enhance T cell recognition of immune-escaped tumors. *J Clin Invest* **126**, 784-794, doi:10.1172/JCI83671 (2016).

15 Doorduijn, E. M. *et al.* T cells specific for a TAP-independent self-peptide remain naive in tumor-bearing mice and are fully exploitable for therapy. *Oncoimmunology* **7**, e1382793, doi:10.1080/2162402X.2017.1382793 (2018).

16 El Hage, F. *et al.* Preprocalcitonin signal peptide generates a cytotoxic T lymphocyte-defined tumor epitope processed by a proteasome-independent pathway. *Proc Natl Acad Sci U S A* **105**, 10119-10124, doi:10.1073/pnas.0802753105 (2008).

17 Durgeau, A. *et al.* Different expression levels of the TAP peptide transporter lead to recognition of different antigenic peptides by tumor-specific CTL. *J Immunol* **187**, 5532-5539, doi:10.4049/jimmunol.1102060 (2011).

18 Martoglio, B. & Dobberstein, B. Signal sequences: more than just greasy peptides. *Trends Cell Biol* **8**, 410-415 (1998).

19 Yewdell, J. W. *et al.* TAP-independent delivery of antigenic peptides to the endoplasmic reticulum: therapeutic potential and insights into TAP-dependent antigen processing. *J Immunother* **21**, 127-131 (1998).

20 Oliveira, C. C. *et al.* New role of signal peptide peptidase to liberate C-terminal peptides for MHC class I presentation. *J Immunol* **191**, 4020-4028, doi:10.4049/jimmunol.1301496 (2013).

21 Blum, J. S., Wearsch, P. A. & Cresswell, P. Pathways of antigen processing. *Annu Rev Immunol* **31**, 443-473, doi:10.1146/annurev-immunol-032712-095910 (2013).

22 Neefjes, J., Jongsma, M. L., Paul, P. & Bakke, O. Towards a systems understanding of MHC class I and MHC class II antigen presentation. *Nat Rev Immunol* **11**, 823-836, doi:10.1038/nri3084 (2011).

23 Kall, L., Krogh, A. & Sonnhammer, E. L. A combined transmembrane topology and signal peptide prediction method. *J Mol Biol* **338**, 1027-1036, doi:10.1016/j.jmb.2004.03.016 (2004).

24 Leonhardt, R. M. *et al.* Post-endoplasmic reticulum rescue of unstable MHC class I requires proprotein convertase PC7. *J Immunol* **184**, 2985-2998, doi:10.4049/jimmunol.0900308 (2010).

25 Leonhardt, R. M., Vigneron, N., Rahner, C. & Cresswell, P. Proprotein convertases process Pmel17 during secretion. *J Biol Chem* **286**, 9321-9337, doi:10.1074/jbc.M110.168088 (2011).

26 Medina, F. *et al.* Furin-processed antigens targeted to the secretory route elicit functional TAP1-/- CD8+ T lymphocytes in vivo. *J Immunol* **183**, 4639-4647, doi:10.4049/jimmunol.0901356 (2009).

27 Tiwari, N. *et al.* A transporter associated with antigen-processing independent vacuolar pathway for the MHC class I-mediated presentation of endogenous transmembrane proteins. *J Immunol* **178**, 7932-7942 (2007).

28 Sette, A. & Sidney, J. Nine major HLA class I supertypes account for the vast preponderance of HLA-A and -B polymorphism. *Immunogenetics* **50**, 201-212 (1999).

29 Sidney, J., Peters, B., Frahm, N., Brander, C. & Sette, A. HLA class I supertypes: a revised and updated classification. *BMC Immunol* **9**, 1, doi:10.1186/1471-2172-9-1 (2008).

30 Andreatta, M. & Nielsen, M. Gapped sequence alignment using artificial neural networks: application to the MHC class I system. *Bioinformatics* **32**, 511-517, doi:10.1093/bioinformatics/btv639 (2016).

31 Nielsen, M. *et al.* Reliable prediction of T-cell epitopes using neural networks with novel sequence representations. *Protein Sci* **12**, 1007-1017, doi:10.1110/ps.0239403 (2003).

32 Mullbacher, A. *et al.* High peptide affinity for MHC class I does not correlate with immunodominance. *Scand J Immunol* **50**, 420-426 (1999).

33 van der Burg, S. H., Visseren, M. J., Brandt, R. M., Kast, W. M. & Melief, C. J. Immunogenicity of peptides bound to MHC class I molecules depends on the MHC-peptide complex stability. *J Immunol* **156**, 3308-3314 (1996).

34 McKee, M. D., Roszkowski, J. J. & Nishimura, M. I. T cell avidity and tumor recognition: implications and therapeutic strategies. *J Transl Med* **3**, 35, doi:10.1186/1479-5876-3-35 (2005).

35 Snyder, J. T., Alexander-Miller, M. A., Berzofskyl, J. A. & Belyakov, I. M. Molecular mechanisms and biological significance of CTL avidity. *Curr HIV Res* **1**, 287-294 (2003).

36 Dutoit, V. *et al.* Heterogeneous T-cell response to MAGE-A10(254-262): high avidity-specific cytolytic T lymphocytes show superior antitumor activity. *Cancer Res* **61**, 5850-5856 (2001).

37 Vigano, S. *et al.* Functional avidity: a measure to predict the efficacy of effector T cells? *Clin Dev Immunol* **2012**, 153863, doi:10.1155/2012/153863 (2012).

38 Anderson, K. S., Alexander, J., Wei, M. & Cresswell, P. Intracellular transport of class I MHC molecules in antigen processing mutant cell lines. *J Immunol* **151**, 3407-3419 (1993).

39 Wei, M. L. & Cresswell, P. HLA-A2 molecules in an antigen-processing mutant cell contain signal sequence-derived peptides. *Nature* **356**, 443-446, doi:10.1038/356443a0 (1992).

40 Uhlen, M. *et al.* Proteomics. Tissue-based map of the human proteome. *Science* **347**, 1260419, doi:10.1126/science.1260419 (2015).

41 Oliveira, C. C. *et al.* Peptide transporter TAP mediates between competing antigen sources generating distinct surface MHC class I peptide repertoires. *Eur J Immunol* **41**, 3114-3124, doi:10.1002/eji.201141836 (2011).

42 Blees, A. *et al.* Structure of the human MHC-I peptide-loading complex. *Nature* **551**, 525-528, doi:10.1038/nature24627 (2017).

43 Lee, Y. K., Menezes, J. S., Umesaki, Y. & Mazmanian, S. K. Proinflammatory T-cell responses to gut microbiota promote experimental autoimmune encephalomyelitis. *Proc Natl Acad Sci U S A* **108 Suppl 1**, 4615-4622, doi:10.1073/pnas.1000082107 (2011).

44 Zitvogel, L., Ayyoub, M., Routy, B. & Kroemer, G. Microbiome and Anticancer Immunosurveillance. *Cell* **165**, 276-287, doi:10.1016/j.cell.2016.03.001 (2016).

45 van Hall, T. *et al.* Selective cytotoxic T-lymphocyte targeting of tumor immune escape variants. *Nat Med* **12**, 417-424, doi:10.1038/nm1381 (2006).

46 Chambers, B. *et al.* Induction of protective CTL immunity against peptide transporter TAP-deficient tumors through dendritic cell vaccination. *Cancer Res* **67**, 8450-8455, doi:10.1158/0008-5472.CAN-07-1092 (2007).

47 Doorduijn, E. M. *et al.* T Cells Engaging the Conserved MHC Class Ib Molecule Qa-1(b) with TAP-Independent Peptides Are Semi-Invariant Lymphocytes. *Front Immunol* **9**, 60, doi:10.3389/fimmu.2018.00060 (2018).

48 Garboczi, D. N., Hung, D. T. & Wiley, D. C. HLA-A2-peptide complexes: refolding and crystallization of molecules expressed in Escherichia coli and complexed with single antigenic peptides. *Proc Natl Acad Sci U S A* **89**, 3429-3433 (1992).

49 Burrows, S. R. *et al.* Peptide-MHC class I tetrameric complexes display exquisite ligand specificity. *J Immunol* **165**, 6229-6234 (2000).

50 Bakker, A. H. *et al.* Conditional MHC class I ligands and peptide exchange technology for the human MHC gene products HLA-A1, -A3, -A11, and -B7. *Proc Natl Acad Sci U S A* **105**, 3825-3830, doi:10.1073/pnas.0709717105 (2008).

51 Harndahl, M. *et al.* Peptide-MHC class I stability is a better predictor than peptide affinity of CTL immunogenicity. *Eur J Immunol* **42**, 1405-1416, doi:10.1002/eji.201141774 (2012).

52 Sanjana, N. E., Shalem, O. & Zhang, F. Improved vectors and genome-wide libraries for CRISPR screening. *Nat Methods* **11**, 783-784, doi:10.1038/nmeth.3047 (2014).

53 Oliveira, C. C. & van Hall, T. Alternative Antigen Processing for MHC Class I: Multiple Roads Lead to Rome. *Front Immunol* **6**, 298, doi:10.3389/fimmu.2015.00298 (2015).

Supplementary figures

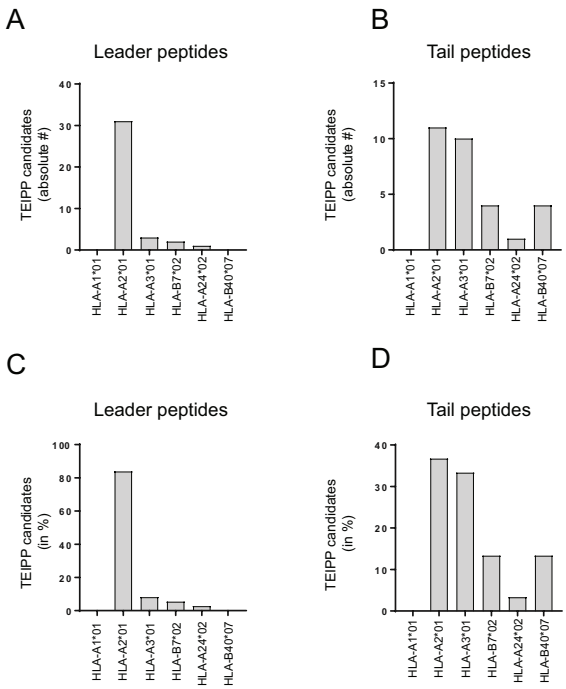

Figure S1. Prediction results of HLA-I binding of TEIPP neoantigen candidates.

TEIPP neoantigen candidate peptides (n=65) were aligned according to HLA binding specificity using a web-based algorithm. (A and B) Absolute number of TEIPP candidates with predicted binding in HLA superclasses for leader peptides and tail peptides. (C and D) Percentage of total TEIPP candidates with predicted binding in HLA superclasses for leader peptides and tail peptides.

A

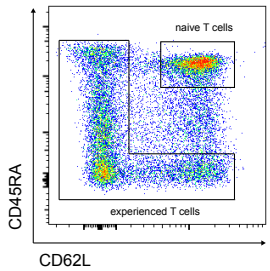

B

Bacteria family name:	peptide sequence
Ruminococcaceae:	TIIKPLIWV
p55:	VIIKPLVWV
Mycobacteriaceae:	LLALAAGLAV
p29:	LLALAAGLAV

C

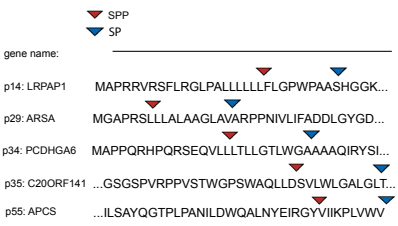

D

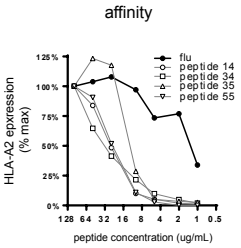

E

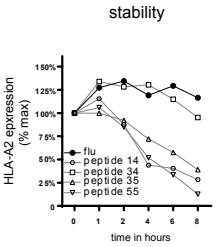

F

p14 TCRs	Vb	p29 TCRs	Vb
1H10	TRBV9	1H12	*
2B1	TRBV28	2G2	*
1A8	TRVB20-1	4D12	*

p34 TCRs	Vb	p35 TCRs	Vb
1G4	TRBV28	1H7	*
1G5	TRBV28	2B3	TRBV28
3G9	TRBV27	5D7	TRBV4

p55 TCRs	Vb
1C2	TRBV17
1E8	TRBV19
2G2	N.D

* unknown Vβ
N.D not determined

Figure S2. Characterization of TEIPP T cells and cognate antigen.

(A) Flow cytometry gating strategy for flow sorting PBMCs into experienced T cells and naive T cells. (B) Overview of bacterial peptide sequences with TEIPP peptide homology. (C) Gene name, peptide sequence, and predicted peptidase cleavage sites (SP [signal peptidase; blue triangle] and SPP [signal peptide peptidase; red triangle]) of p14, p29, p34, p35, and p55. (D) pHLA peptide affinity was measured by a cellular-based assay. Percentage of maximum HLA-I expression was determined by flow cytometry to calculate EC50 values. (E) pHLA peptide stability was measured by calculating EC50 values of maximum HLA-I expression over time. (D and E) Representative data of four independent experiments are shown. (F) Multiple T cell clones with different Vβs for the different specificities were isolated. Shown are the T cell clone name and corresponding T cell receptor β variable gene name, determined by using a TCR Vβ Screening Kit analyzed by flow cytometry

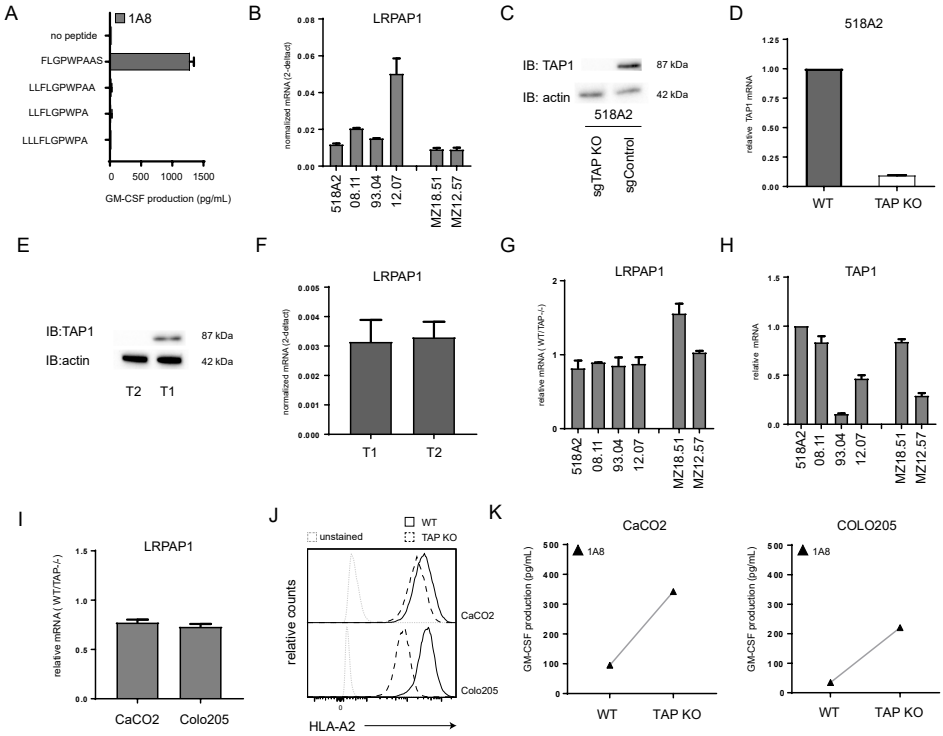

Figure S3. mRNA and protein expression analysis on tumor panel.

(A) Peptide specificity of the LRPAP121-30-specific T cell clone 1A8 was assessed by testing different length variants of the p14 peptide at different locations of the signal peptide. Peptides with a predicted HLA-A*02:01 binding (IC50 < 500 nM) were tested. GM-CSF cytokine production was measured by ELISA. (B) LRPAP1 mRNA levels of the tumor panel were determined by qPCR. (A and B) Data are shown as mean ± SD; n = 3. (C) TAP1 protein levels of the 518A2 skin melanoma cell line variants were measured using Western blot. No TAP1 expression was observed in the 518A2 TAP KO variant. (D) mRNA expression of TAP1 gene of the 518A2 skin melanoma cell line variants was determined by qPCR. Data are shown as mean ± SD; n = 2. (E) TAP1 protein levels of the T1 and T2 lymphoma were measured using Western blot. No TAP1 expression was observed in the T2 lymphoma. (F) LRPAP1 mRNA expression levels of the T1 and T2 lymphoma were determined by qPCR. Both cell lines had equal LRPAP1 mRNA expression. Data are shown as mean ± SD; n = 2. (G) LRPAP1 mRNA expression levels of the tumor panel were examined by qPCR. Relative mRNA gene expression of the TAP KO variant compared with WT variant was calculated. (H) Relative TAP1 mRNA levels of the tumor panel were determined by qPCR. (G and H) Data are shown as mean ± SD; n = 3. (I) LRPAP1 mRNA expression levels of two colon carcinoma cell lines were determined by qPCR. Equal levels of LRPAP1 mRNA expression were observed. Data are shown as mean ± SD; n = 2. (J) HLA-A*02:01 surface expression of the antigen-processing machinery–impaired colon carcinoma lines were measured by flow cytometry. (K) GM-CSF production of T cell clone 1A8 upon antigen recognition of two colon carcinomas (WT versus TAP KO). (J and K) Representative data of two independent experiments are shown.

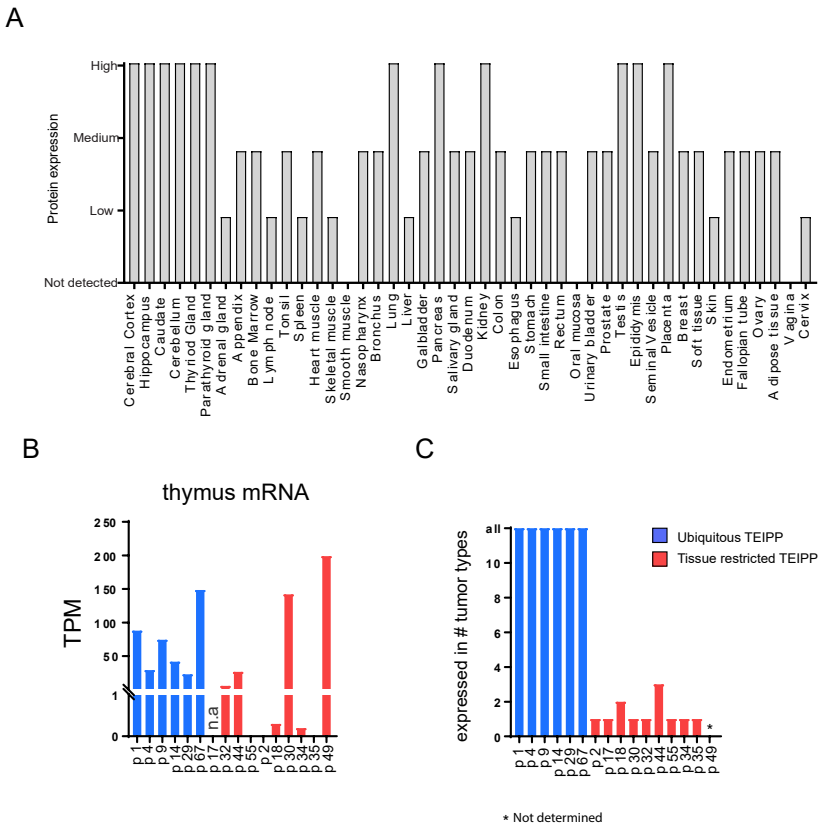

Figure S4. Database analysis of TEIPP candidates.

(A) LRPAP1 protein expression in 44 different healthy tissues. Data collected from the Human Protein Atlas. (B) mRNA expression of 16 identified TEIPP antigens in the thymus, expressed in tags per million (TPM). Data collected from FANTOM5 datasets. n.a., not applicable. (C) mRNA expression data of the TEIPP antigens were of different tumor types and were extracted from the Cancer Genome Atlas database. Our list with 16 TEIPP antigens is categorized in two groups: ubiquitous TEIPP, all examined tumor types have mRNA expression of the respective TEIPP antigen (TPM > 5); and tissue-restricted TEIPP, mRNA expression was only detected in some tumor types (TPM > 5).

Table S1. Overview of peptidome analyses from human tumor samples

Tissue Type	Malignant / Benign	n
Bone Marrow Mononuclear Cells	Benign	10
Granulocytes	Benign	2
PBMC	Benign	30
Liver	Benign (adjacent to tumor)	12
Colon	Benign (adjacent to tumor)	35
Ovary	Benign (adjacent to tumor)	4
Kidney	Benign (adjacent to tumor)	27
AML	Malignant	19
Breast Cancer	Malignant	2
CLL	Malignant	32
CML	Malignant	16
Glioblastoma	Malignant	6
HCC	Malignant	12
CRC	Malignant	35
Leiomyosarcoma	Malignant	1
Merkel Cell Carcinoma	Malignant	1
Meningioma	Malignant	1
Multiple Myeloma	Malignant	9
NSCLC	Malignant	1
Ovarian Cancer	Malignant	35
Peritoneal Carcinomatosis	Malignant	1
Polycythemia vera	Malignant (pre-)	10
RCC	Malignant	31
T-ALL	Malignant	2
Cell lines	Malignant / Immortalized	17
Total	Malignant	231
	Benign	120